Proceedings of the 10th World Congress on Momentum, Heat and Mass Transfer (MHMT 2025)
Barcelona, Spain - April, 2025
Paper No. ENFHT 179
DOI: 10.11159/enfht25.179

Development of a Bioinspiration Search Method for Thermal Design

Thomas Slavens[1], Hamidreza Shabgard[1]
[1]College of Aerospace and Mechanical Engineering, University of Oklahoma
865 Asp Ave. Norman, OK 73019 USA
tslavens@ou.edu; shabgard@ou.edu

Abstract – This paper describes a novel means to search for bioinspired cooling design features. With the advent of advanced free-form manufacturing methods such as DMLS or FDM printing, new and novel design structures can be deployed taking advantage of biomimetic and bioinspired structures. While structural and aerodynamic biomimetic structures have been readily leveraged to design problems, the acquisition and integration of bioinspired cooling structures has lagged within thermal design. The method developed hypothesises that the broadness of a species operative temperature range can be used to highlight species that may have phenotypic plasticity allowing for within-species adaptions to local thermal conditions. To demonstrate this hypothesis, the method is executed using ERA5 Land climate data to calculate an operative temperature across the continental United States. The operative temperature is based on a 1D heat balance of a massless exposed surface which includes effects of radiation and convective heat transfer to the environment. The resultant operative temperatures were then mapped onto the North American tree basal distributions and each species operative temperature range was evaluated. Results of this mapping showed little correlation between operative temperature variation with spatial distribution of species along latitude and longitude gradients and no correlation was observed to the average catalogued leaf width of the species in this study. These results indicate other mechanisms may be stronger drivers to tree thermal range capacity and points to opportunities in detailed morphological and physiological studies of top ranked species. These structures can then be abstracted and included into bioinspiriation databases and thermal design systems.

***Keywords*:** bioinspiration, cooling design, heat transfer, operative temperature, environmental heat transfer

1. Introduction

The development of systems that allow for efficient execution of engineering design work is an important part of most corporate knowledge architectures. With the advent of more ‘free-form’ manufacturing technologies such as additive manufacturing, design spaces from older calcified design systems act to limit the variations pursued by design engineers. Having design methods that incorporate available new design space is critical during concept design which focusses on the development of a basic solution of the problem through the elaboration of a solution principle [1]. A popular subset of creative design, biomimetics, leverages biological information for the development of novel solutions. Biomimetics is the study of biological mechanisms for the development of similar solutions by artificial means [2]. Differing degrees of biomimetic design exist: biomorphism aims to copy biological mechanisms within engineered products to solve a similar problem as the biological system. Bioinspiration aims to leverage biological mechanisms for use in solutions adjacent to the intent of the adaption [3]. The process of utilizing bioinspiration establishes a correlation of ideas between the problem being addressed and observed solutions in nature taking advantage of “nature’s genius” [4]. It has been shown that introduction of possible similar biological systems during the ideation phase of concept design can lead to the introduction of more novel design solutions [5].

A major hurdle in the use of bioinspiration is collecting, assessing, and leveraging biological solutions within the design process. A major gap encountered is association between biological systems and their utility to out-of-domain design problems [6]. A number of solutions have been implemented to solve this gap through databases or document crawls [7]. For these systems to be of use, they need to be pre-populated with translations to in domain solutions. Reviews of additive-enabled biomimetic design regularly feature bio-optimized designs for structural and aerodynamic applications [4] [8]. However, few works exist on leveraging biomimetic features for the design of single-phase cooling structures for heat transfer. While a major facet of most biological systems, it is a difficult to systematically isolate organism features evolved that have been readily optimized for this activity.

A means to systematically search for this adaptive behaviour is to investigate morphological changes within species structures across environmentally distinct locations. For heat transfer this would be environments with different heat loading.

Graduated adaptions of a species within an environmental gradient are defined as *clines* [9]. This graduated adaption is a consequence of the *Phenotypic Plasticity* response of an organism to biotic or abiotic factors (such as thermal heat load) through changes in characteristics or behaviour [10] [11] [12] [13]. Investigating this phenotypic plastic response over a thermal cline provides a systematic means to search for structures of useful nature to heat transfer design.

The work of this paper seeks to develop a framework to systematically investigate species for thermally adaptive structures of interest. The goal of this paper is (1) to develop a singular heat load metric of merit to describe the thermal range of a species taking into account radiation and environmental loading, (2) identify first-order trends of this metric, and (3) identify direction for future work. The study region is framed within the continental United States with leaf structures if North American tree species of interest. This builds on similar research by [14] where they investigated lobe variation of within-tree leaf variation (between sun and shade leaves of a single tree) to develop passive evaporative cooling structures. This research takes a broader view incorporating variation of leaves along a thermal cline developed from Toposcale climate data. In this manner, trees with an exposure to a larger range of temperature will provide a down-selection of species and structures from which a heat transfer configuration solution could be developed.

2. Methods

2.1. Development of the Thermal Metric: Operative Temperature

To investigate morphological variations of tree species leaves along a thermal cline, development of a heat load factor that takes into account different modes of heat transfer into a leaf must be developed. This thermal heat load factor is intended to serve as a single parameter surrogate to describe the thermal load encountered by species across their basal region. While air temperature is the most readily available climatic factor to characterize the temperature environment of an organism it does not capture the multiple modes of energy transfer that occurs at the interface between it and the environment. Early developments of climatic factors that tried to more holistically capture the heat necessary for vegetation development utilized summation of days above a certain critical temperature or the summation of temperatures over a specific time period [15]. These climatic factors incorporated a sum of daily average temperatures as a proxy for the amount of heat load incident on a plant in lieu of direct measurements of incident radiation which modern climate datasets provide.

A rationale index of interest, *operative temperature* (T_o), was introduced by Winslow [16] incorporating the heat balance from reclined subjects within an enclosed space with turbulent air flow. *Operative temperature* does not define a measurable parameter, but is a scale dependent on the thermal demands of the environment on an organism [16]. The operative temperature is the resultant temperature of an organism in consideration of the energy transfer between it and the environment. The environment transfers energy to and from an organism by convection (by both single phase transfer to the air and multiphase transfer through transpiration), radiation (due to solar radiation and emittance), and conduction into surfaces it contacts [17]. A diagram of pertinent heat transfer mechanisms impacting the temperature of plants is shown in Figure 1. Here three modes of radiation heat transfer are identified showing direct solar insolation (predominantly short-wave radiation), atmospheric thermal radiation due to emission from aerosols and clouds within the atmosphere (long-wave radiation), and radiative emission from the plant itself.

Convection heat transfer is identified in Figure 1 along with leaf transpiration. Transpiration is the process of water loss from a plant through evaporation through stomata pores from aerial parts of the plants such as leaves, stems, and flowers [18]. Transpiration rates vary during a diurnal cycle, are impacted by wind effects and humidity, and are passively controlled by stomata in response to light, CO_2 concentrations, temperature and water availability [19] [20] [21]. Due to the complexity of accounting for the transpiration behaviour of leaves, this mechanism was ignored to plainly focus on the heat load encountered by leaves. A marginal amount of heat transfer is also caused by conduction between the plant and the soil. With the focus of the search being leaf morphologies, this minor conduction away from the leaves can also be ignored [18]. Further, the organism is assumed to be at a steady state condition where changes in body temperature can be ignored.

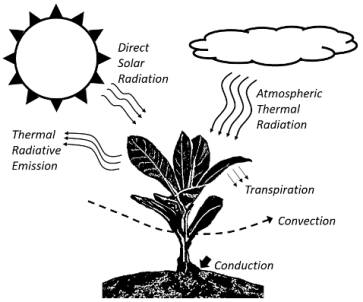

Figure 1: Modes of heat transfer impacting tree leaf temperature

Given these mechanisms of heat transfer, a heat balance of a leaf treated as a massless system can be derived as:

$$0 = \dot{Q}_{sw} + \dot{Q}_{LW} + \dot{Q}_{em} + \dot{Q}_{conv} \qquad (1)$$

Here $\dot{Q}_{sw}$ is the incident solar *short wave* radiation, $\dot{Q}_{LW}$ the incident thermal *long wave* radiation, $\dot{Q}_{em}$ the radiative emission, and $\dot{Q}_{conv}$ the convective heat transfer the surrounding air. Equation (1) can be solved to determine an operative temperature of a target organism. Radiation loads Q_{SW} and Q_{LW} can be calculated from empirical methods, taken from site measurements, or from climate models. Using Newton's law of cooling for $\dot{Q}_{conv}$ and radiation loss $\dot{Q}_{em}$ from the Stefan-Boltamann law of radiation, (1) can be re-written as:

$$0 = \dot{Q}_{sw} + \dot{Q}_{LW} + \sigma \cdot \varepsilon \cdot A \cdot T_o^4 + h \cdot A \cdot (T_a - T_o) \quad (2)$$

Here h is the convective heat transfer coefficient, A the area exposed to convection, T_a the atmospheric free-stream temperature, σ is the Stefan-Boltzmann constant (5.67e-8 J/s*m^2*k^4), ε is the emissivity of the leaf, and T_o the surface temperature or *operative temperature* of the leaf. Equation (2) is then solved to approximate the operative temperature of an organism at a given location and serve as our thermal heat load factor.

2.2. Climate Data Set

To calculate the operative temperature, ERA5-Land data is used from 1970 to 2000 on a 0.08° x 0.08° degree grid (representing a grid size of roughly 9 km equatorially) on an hourly basis [22]. This provides a thirty year data set consistent with typical recommendations for climate calculations [23]. This dataset incorporates ERA5 atmospheric reanalysis (based on reanalysis of station and satellite data) to feed the ECMWF land surface model to describe the exchanges of global energy, water, and carbon fluxes on the land surface [24]. The land model takes into account atmospheric elevation, open water status within the grid, vegetation, and snow cover to assess the transport of energy and water at each grid point utilizing the ERA5 atmospheric data as inputs into the model balances. The dataset provides parameters of interest to equation (2): 2-meter air temperature (t2m), wind speeds (v_a), surface solar radiation downwards (ssrd), surface solar radiation downwards (strd), and surface pressure (sp). Note the radiation values are the total flux incident to a surface parallel with the local surface of the earth. The hourly data is given starting from UTC and is shifted to align to local noon of the study location.

2.3. Operative Temperature Calculation

For the calculation of equation (2), it was assumed that heat transfer was occurring across a uniformly 3 cm wide leaf, perpendicular to incoming radiation, and under a cross draft equal to v_a as illustrated in Figure 2. Solar heat fluxes from the ERA5-Land dataset were directly used in the solution of equation (2).

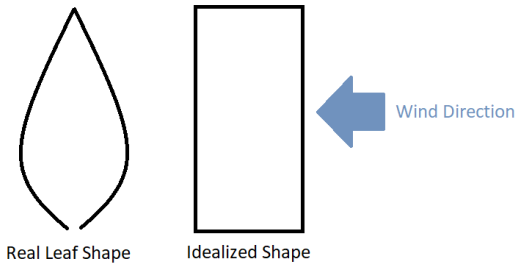

Figure 2: Comparison of a real leaf shape to the idealized shape used for operative temperature calculation.

An empirical correlation of the average Nusselt number across a flat plate under laminar flow conditions was used. Laminar flow was assumed in that a majority of the flow regimes processed were laminar in nature and reflected the worst outcomes in terms of cooling efficiency. The correlation assumed was based on a flat plate correlation as described in [25]:

$$Nu = 0.68 \cdot Re^{0.5} \cdot Pr^{0.33} \qquad (5)$$

A bi-section iterative solution method was developed for equation (2) iterating on the error in attaining zero on summing each of the heat flux modes acting on the ideal leaf. Convergence criteria was heat flux error of 0.001 W/m^2. The

radiation model of equation (2) assumes an emissivity of 0.98 with the range reported for typical leaf values [18] [26] [27] under solar wavelength shortwave radiation.

On each day of the year, the max, min, and average operative temperatures were calculated and then averaged over the data range to give an average of these operative temperature metrics for a given day. The maximum operative temperature was then aggregated across the year to provide the maximum operative temperature of the species range. Results of this monthly aggregation is shown in Figure 3 for the month of June. Here the maximum monthly air, operative temperature, and their difference are shown for the study region highlighting the impact of radiation load on operative temperatures of the species. This inclusion increases the subject's surface temperature relative to the ambient air temperature across the entirety of the study region with the highest impacts noted in southern latitudes and high elevation regions.

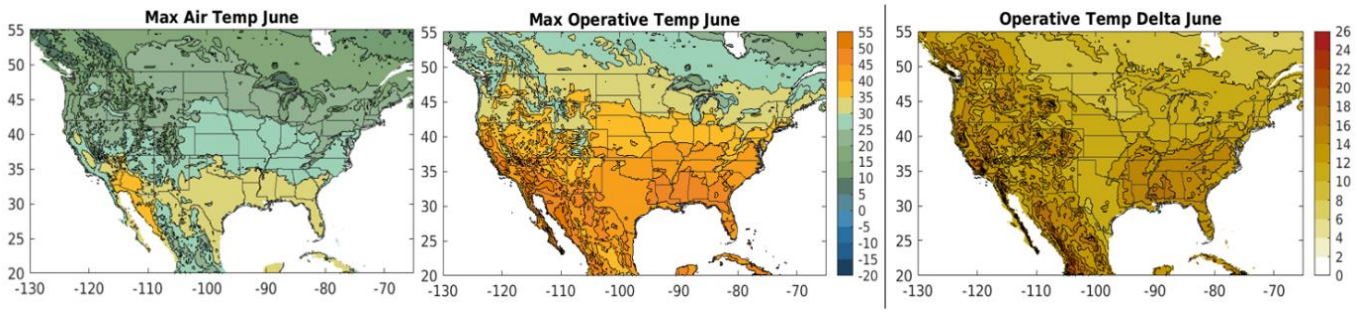

Figure 3: Average daily maximum operative temperatures for June from 1970 to 2000

For the basal locations of trees of North America, a digital representation of the "Atlas of United States Trees" by Elbert L. Little, Jr. was utilized [28]. This atlas represents the natural distribution of different tree species within North America ignoring expansions of the regions to where they may have been transplanted. This dataset provides the spatial connection between species distribution and the climate range from which it experiences. The dataset was mapped to the ERA5-Land grid and the existence of the 679 species of tree were recorded as a logical flag within the map grid. Due to the mismatch in grid fidelity between the ERA5 dataset and the basal location dataset, a clustering algorithm was used to isolate major contiguous points in operative temperature space. This algorithm was used to eliminate edge-based false positives which would attribute significantly different climate data to typical species niches. The operative temperature range of the species were then calculated based on the maximum and minimum encountered temperatures spatially. An example for the T_o range determination for a species is shown for *Quercus palustris* (Spanish oak) in Figure 4. This species has a distribution range between 35 to 45 degrees latitude and from -75 to -95 degrees longitude. The maximum T_o of the range is identified to be 49°C and the minimum at the northern latitudes found to be 25°C, the difference of these being approximately 24°C. This difference is recorded as the *maximum operation temperature* range of this species.

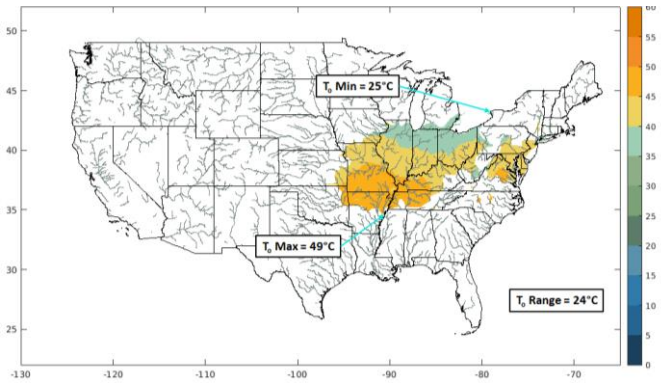

Figure 4 Maximum operative temperature over the basal range of species Quercus palustris (Spanish Oak).

3. Results

3.1. Operative Temperature Rankings

Calculations of operative temperature were carried out for all 679 species contained within the Atlas data.. In the final function of the process, the species were ranked by the range of maximum operative temperature across the observed thermal cline. These results are shown in Table 1 for the top five species. These results show the maximum and minimum maximal

operative temperature across the thermal cline along with the characteristic width of the leaf as cited in [29] and [30]. This ranking will be used to isolate species of interest for thermal adaptions in further works. The largest maximum operative temperature spread of Salix exigua tops out at nearly 35°C for the basal range of this species while the average and median values of the species in Table 1 is 24.2°C and 23°C respectively.

Table 1: The top four tree species ranked by maximum operative temperature range post cluster screening.

Tree Species	Maximum Operative Temperature (°C)	Minimum Operative Temperature (°C)	Operative Temperature Range (°C)	Characteristic Leaf Width (mm)
Salix exigua	58.7	23.0	35.7	9.0
Prunus pensylvanica	46.2	17.1	29.1	26.0
Salix lasiandra	51.2	22.8	28.5	20.0
Prunus virginiana	50.0	23.0	27.0	37.5

Operative temperature distribution maps of the top four species with the highest operative temperature range is shown in Figure 5. All four species show spatial continuity from Canada to roughly 30-35° latitude. Outside of Salix exigua and to some extent Prunus virgiana, exposure to elevated operative temperatures occurs along narrow extents of the species following along mountain ranges. This distribution may indicate that the species is adapted to a climate whose over-all average is cooler driving a proclivity to either northern latitudes or a higher altitude regime where the composite maximums shown here are only short-lived with adequate hydration to allow cooling during these short bursts.

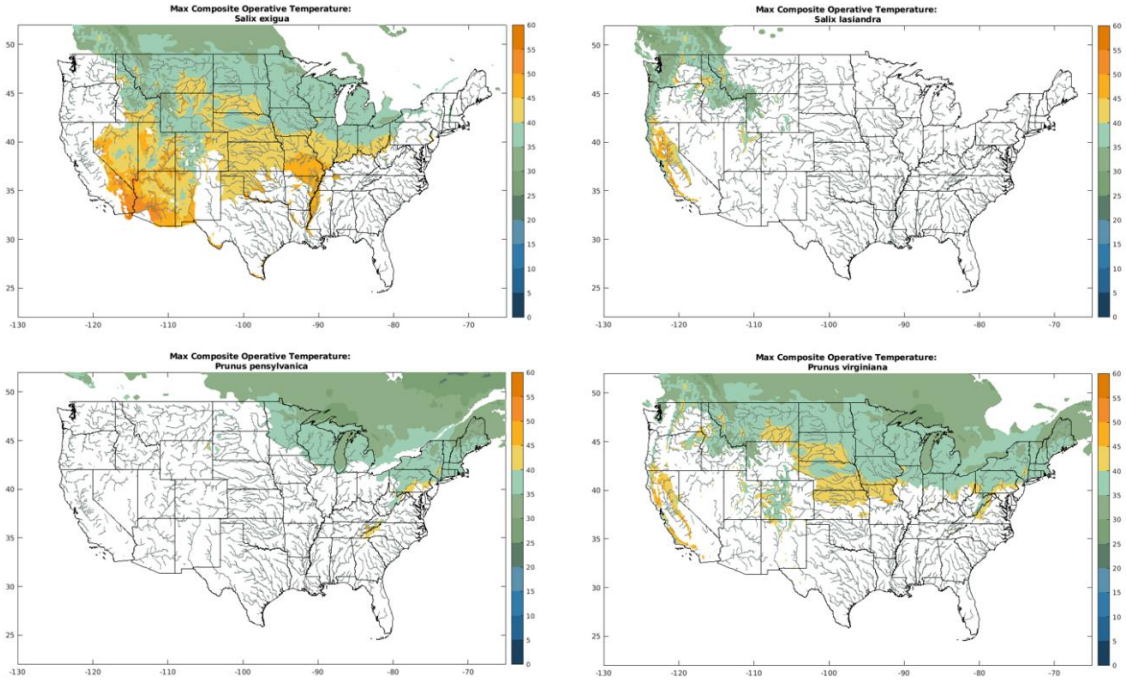

Figure 5 Spatial and maximum operative temperature distributions of for Salix exigua, Prunus pensylvanica, Salix lasiandra, and Prunus virginiana.

3.2. Key Parameter Trends

From the thermal niche distributions shown in Figure 5, it can be observed that the operative temperatures seen by a species is strongly tied to the spatial distribution of the species. Linear regression analysis of the operative temperature over the thermal niche of the Atlas species was conducted for variation along both latitudinal and longitudinal gradients. Figure 6 shows the breakdown of species operative temperature variation with latitude. For both minimum and maximum operative temperatures, it shows that a majority of the species (>50%) have low variation of operative temperature to latitude. Those with high correlation to latitude (such as Plot C of Figure 6) have an observed gradient as the species moves from higher to lower latitudes. Variation of operative temperatures to longitude is shown in Figure 7. Here the correlation is much weaker with a large majority (>60%) of species having little variation of operative temperature across longitudes.

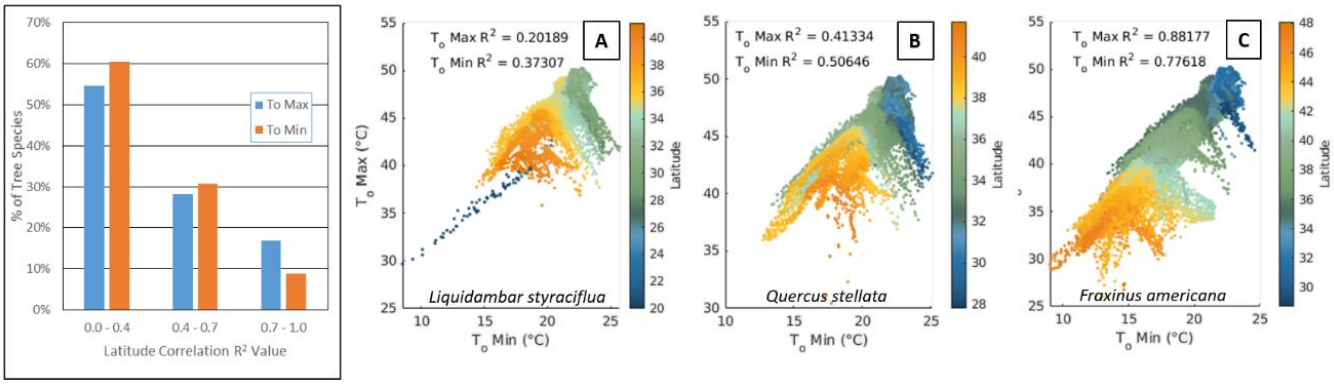

Figure 6: Regression analysis of the variation of species operative temperature to latitude. Histogram on the left shows the breakdown of response of the study species indicating only a small percentage showed strong operative temperature trend to latitude. Plots A, B, and C are examples showing three species exhibiting low (plot A), moderate (plot B), and high (plot C) T_o correlation to latitude gradient.

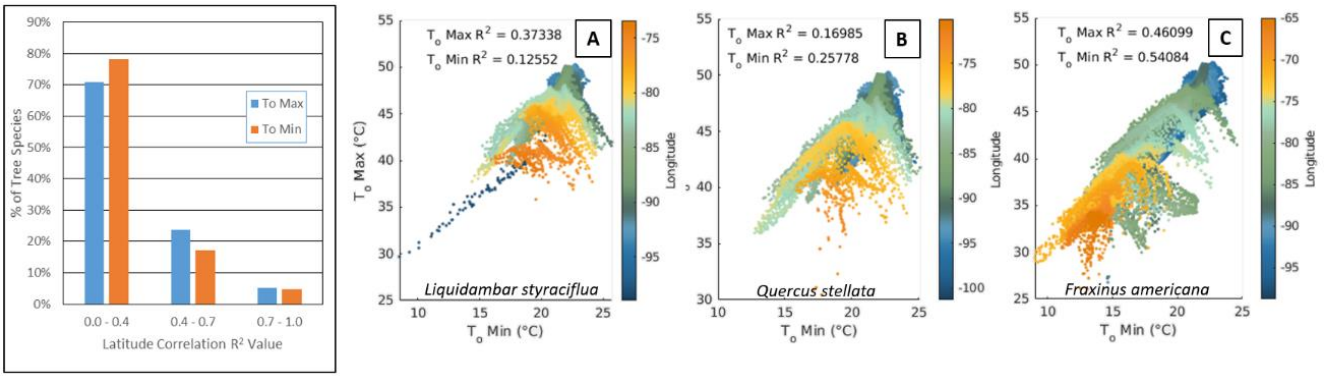

Figure 7: Regression analysis of the variation of species operative temperature to longitude. Histogram on the left shows the breakdown of response of the study species indicating only a small percentage showed strong operative temperature trend to longitude. Plots A, B, and C are examples showing three species exhibiting low (plot A), moderate (plot B), and high (plot C) T_o correlation to longitude gradient.

Variation of leaf width to maximum operative temperature range is shown in Figure 8. The linear regression assessment shows very little correlation between the maximum operative temperature range and the average leaf width for the species. While indicating that a gross width of leaf does not indicate correlation to a large breadth of thermal robustness, it does not rule out that this may be a cogent parameter that is varied by phenotypic plasticity based on the region of growth's environmental conditions. This results points out that in-depth investigations on species may be needed to unravel how a species may vary along their operative thermal niche.

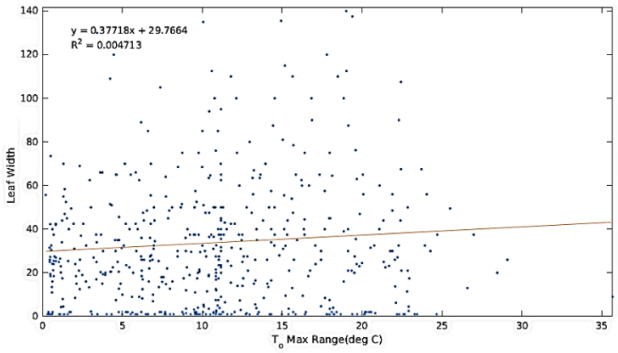

Figure 8: Variation of leaf width (mm) as a function of maximum operative temperature range. Regression shows little correlation between operative temperature range and leaf width.

3.2. Discussion of Results

The operative temperature model used for this study represents an idealized estimate of the heat load a leaf may be exposed to during the day. Further, the calculation through the diurnal data sets provide heat loss estimates during the night time hours. An estimate of the resultant operative temperatures provides insights into the magnitude of heat that a characteristic leaf needs to accommodate to reside in a preferred temperature range for photosynthesis. Keeping in mind a general average optimum leaf temperature of approximately 33°C [31], the maximum operative temperature results show that unmitigated surface heat-up beyond 20°C as observed in Figure 3. This temperature delta is managed by adaptions to (1) operate at higher temperature regimes or (2) provide cooling means such as evaporative cooling where local moisture content sustains it or augmentation to convection to the atmosphere when moisture is limited. It is the latter mechanism which provides interest in biomimetic inspiration for cooling augmentation.

The results of Table 1 and Figure 5 highlight the operative temperature metric's ability to highlight species with thermal clines across large thermal environment regimes. The method tends to highlight species with large spatial distributions dominated through a significant latitudinal distribution. However, the regression analysis shown in FiguresFigure 6 andFigure 7 indicates that latitude is not a strong driver to the maximum operative temperatures encountered by a species. This would imply that many species tend to follow similar thermal environments along latitudinal and longitudinal space. Hallmarks of this behaviour is observed in the species Salix lasiandria and Prunus pensylvanica of Figure 5. Both species are predominantly cool weather species and have southerly excursions that map along mountain ranges. Their high operative temperature range highlights a short-fall in the calculation in that the calculation represents heating in lieu of any transpiration cooling that a leaf would use. Incorporation of this parameter would need further calibration to field observations to understand the variation in transpiration in relationship to the availability of water in a region.

4. Conclusion

In this work, a novel method to evaluate the thermal loading tree species may be encounter was developed using a 1-D heat flux model based on a 3 cm wide black body flat plate with no temperature mass. This idealized system was used to estimate exposed surface temperatures of generic model leaf under the loads of solar radiation, air convection, and radiative heat loss. Utilizing ERA5 Land climate data over 24 hour periods, the maximum, minimum, and average yearly operative temperature across the continental United States was calculated and mapped onto the basal distribution of North American tree species. The maximum operative temperature range of the species were then calculated allowing for a ranking of species based on breadth of thermal loading within their habitat. Assessment of this parameter showed that a wide operative temperature range does not correlate to average leaf width nor do the majority of species operative temperatures vary significantly against latitude and longitude. These results indicate that other factors may be stronger drivers to thermal breadth necessitating (1) inclusion of local moisture contribution via transpiration or (2) higher fidelity studies into individual species of interest as highlighted in the ranked list.

In future work, species highlighted by this search mechanism will be investigated for morphological variation along these thermal clines. These morphologies will be evaluated for their impact to heat transfer and incorporated into cooling designs as a demonstration of the full arch of leveraging this method in a typical design system.

References

[1] G. Pahl, W. Beitz, J. Feldhusen and K. Grote, Engineering Design: A Systematic Approach, London: Springer-Verlag, 2007.

[2] J. F. Vincent, "Biomimetics—a review," *Proceedings of the institution of mechanical engineers, part H: Journal of Engineering in Medicine,* vol. 223, no. 8, pp. 919-939, 2009.

[3] C. Santulli and C. Langella, "Introducing students to bio-inspiration and biomimetic design: A workshop experience," *International Journal of Technology and Design Education,* vol. 21, no. 4, pp. 471-485, 2011.

[4] A. du Plessis, C. Broeckhoven, I. Yadroitsava, I. Yadroitsev, C. Hands, R. Kunju and D. Bhate, "Beautiful and functional: a review of biomimetic design in additive manufacturing," *Additive Manufacturing,* vol. 27, pp. 408-427, 2019.

[5] J. O. Wilson, D. Rosen, B. A. Nelson and J. Yen, "The effects of biological examples in idea generation," *Design Studies,* vol. 31, no. 2, pp. 169-186, 2010.

[6] K. Wanieck, P.-E. Fayemi, N. Maranzana, C. Zollfrank and S. Jacobs, "Biomimetics and its tools," *Bioinspired, Biomimetic and Nanobiomaterials,* vol. 6, no. 2, pp. 53-66, 2017.

[7] K. Fu, D. Moreno, M. Yang and K. L. Wood, "Bio-inspired design: an overview investigating open questions from the broader field of design-by-analogy," *Journal of Mechanical Design,* vol. 136, no. 11, p. 111102, 2014.

[8] Y. Yang, Z. Li, Z. Chen, C. Zhou, Q. Zhou and Y. Chen, "Recent progress in biomimetic additive manufacturing technology: from materials to functional structures," *Advanced Materials,* vol. 30, no. 36, p. 1706539, 2018.

[9] J. Huxley, "Clines: an auxiliary taxonomic principle," *Nature,* vol. 142, no. 3587, pp. 219-220, 1938.

[10] T. J. DeWitt, A. Sih and D. S. Wilson, "Costs and limits of phenotypic plasticity," *Trends in ecology & evolution,* vol. 13, no. 2, pp. 77-81, 1998.

[11] A. A. Agrawal, "Phenotypic plasticity in the interactions and evolution of species," *Science,* vol. 294, no. 5541, pp. 321--326, 2001.

[12] D. Whitman, Phenotypic plasticity of insects: mechanisms and consequences., Science Publishers, Inc., 2009.

[13] C. K. Ghalambor, J. K. McKay, S. P. Carroll and D. N. Reznick, "Adaptive versus non-adaptive phenotypic plasticity and the potential for contemporary adaptation in new environments," *Functional Ecology,* vol. 21, no. 3, pp. 394-407, 2007.

[14] P. Gruber and A. Rupp, "Investigation of leaf shape and edge design for faster evaporation in biomimetic heat dissipation systems," *Bioinspiration, Biomimetics, and Bioreplication VIII,* vol. 10593, pp. 118-133, 2018.

[15] S. Tuhkanen, Climatic parameters and indices in plant geography, Acta Phytogeographica Suecica 67, 1980.

[16] C. E. Winslow, L. P. Herrington and A. P. Gagge, "Physiological reactions of the human body to varying environmental temperatures," *American Journal of Physiology-Legacy Content,* vol. 120, no. 1, pp. 1-22, 1937.

[17] G. S. Bakken, W. R. Santee and D. J. Erskine, "Operative and standard operative temperature: tools for thermal energetics studies," *American Zoologist,* vol. 25, no. 4, pp. 933-943, 1985.

[18] D. M. Gates, "Transpiration and leaf temperature," *Annual Review of Plant Physiology,* vol. 19, no. 1, pp. 211-238, 1968.

[19] B. G. Drake, K. Raschke and F. B. Salisbury, "Temperature and transpiration resistances of Xanthium leaves as affected by air temperature, humidity, and wind speed," *Plant Physiology,* vol. 46, no. 2, pp. 324-330, 1970.

[20] P. G. Jarvis and K. G. McNaughton, "Stomatal control of transpiration: scaling up from leaf to region," *Advances in ecological research,* vol. 15, pp. 1-49, 1986.

[21] H. Meidner and T. A. Mansfield, Physiology of Stomata, Maidenhead, England: McGraw-Hill Publishing Company Limited, 1968.

[22] J. Munoz-Sabater, E. Dutra, A. Agusti, C. Albergel, G. Arduini, G. Balsamo, S. Boussetta, M. Choulga, S. Harrigan, H. Hersbach, B. Martens, D. Miralles, M. Piles, N. Rodriguez, E. Zsoter, C. Buontempo and J. Thepaut, "ERA5-Land: a new state-of-the-art global land surface reanalysis dataset," *Earth Syst. Sci. Data,* vol. 13, pp. 4349-4383, 2017.

[23] E. Linacre, Climate data and resources: a reference and guide, Routledge, 2003.

[24] S. Boussetta, G. Balsamo, G. Arduini, E. Dutra, J. McNorton, M. Choulga, A. Agusti, A. Beljaars, N. Wedi, J. Munoz-Sabater, P. de Rosnay, I. Sandu, I. Hadade, G. Carver, C. Mazzetti, C.

Prudhomme, D. Yamazaki and E. Zsoter, “ECLand: The ECMWF Land Surface Modelling System,” *Atmosphere,* vol. 12, no. 6, p. 723, 2021.

[25] J. L. Monteith and M. H. Unsworth, Principles of Environmental Physics: Plants, Animals, and the Atmosphere, Oxford: Elsevier Ltd., 2013.

[26] A. D. Richardson, D. M. Aubrecht, D. Basler, K. Hufkens, C. D. Muir and L. Hanssen, “Developmental changes in the reflectance spectra of temperate deciduous tree leaves and implications for thermal emissivity and leaf temperature,” *New Phytologist,* vol. 229, no. 2, pp. 791-804, 2021.

[27] C. Chen, “Determining the leaf emissivity of three crops by infrared thermometry,” *Sensors,* vol. 15, no. 5, pp. 11387--11401, 2015.

[28] E. L. Little and L. A. Viereck, Atlas of United States Trees, US Government Printing Office, 1971.

[29] C. F. Brockman, A Guide to Field Identification: Trees of North America, Racine, WI: Golden Press, 1979.

[30] A. J. Coombes, The Book of Leaves, East Sussex, UK: Ivy Press, 2010.

[31] E. Linacre, “A note on a feature of leaf and air temperatures,” *Agricultural Meteorology*, vol. 1, no. 1, pp. 66--72, 1964.